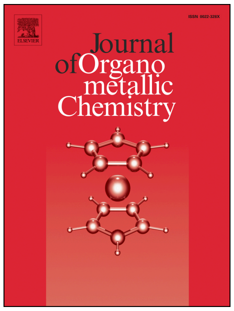

Dehydrogenative coupling of alcohols to esters on a silica polyamine composite by immobilized PNN and PONOP pincer complexes of ruthenium

Md Abdul Goni, Edward Rosenberg, Roberto Gobetto, Michele Chierotti

PII: S0022-328X(17)30331-5

DOI: 10.1016/j.jorganchem.2017.05.036

Reference: JOM 19962

To appear in: *Journal of Organometallic Chemistry*

Received Date: 27 February 2017

Revised Date: 14 May 2017

Accepted Date: 17 May 2017

Please cite this article as: M.A. Goni, E. Rosenberg, R. Gobetto, M. Chierotti, Dehydrogenative coupling of alcohols to esters on a silica polyamine composite by immobilized PNN and PONOP pincer complexes of ruthenium, *Journal of Organometallic Chemistry* (2017), doi: 10.1016/j.jorganchem.2017.05.036.

Graphic for:

Dehydrogenative Coupling of Alcohols to Esters on a Silica Polyamine Composite by Immobilized PNN and PONOP Pincer Complexes of Ruthenium

by

Md Abdul Goni and Edward Rosenberg[*]

Department of Chemistry and Biochemistry, University of Montana, Missoula MT 59812

and

Roberto Gobetto and Michele Chierotti

Dipartimento di Chimica IFM, Universitá di Torino, via P. Giuria 7, 10125,Turin, Italy

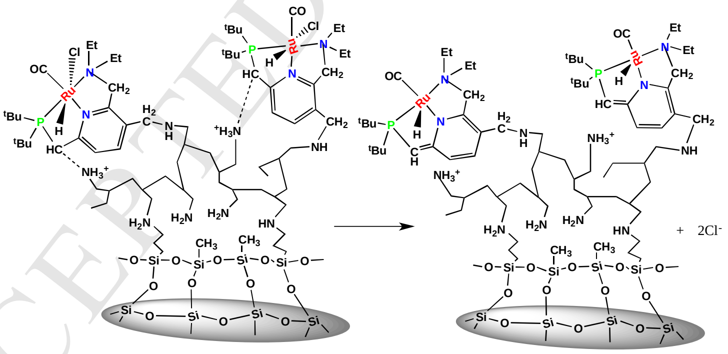

Dehydrogenative Coupling of Alcohols to Esters on a Silica Polyamine Composite by Immobilized PNN and PONOP Pincer Complexes of Ruthenium

by

Md Abdul Goni and Edward Rosenberg*

Department of Chemistry and Biochemistry, University of Montana, Missoula MT 59812

and

Roberto Gobetto and Michele Chierotti

Dipartimento di Chimica IFM, Universitá di Torino, via P. Giuria 7, 10125,Turin, Italy

Abstract

Heterogenization of catalytically important homogeneous catalysts on solid supports has become an expanding area of research. PNN and PONOP ruthenium pincer complexes were immobilized on a silica poly(allylamine) composite, BP-1 by a two-step Mannich reaction. The complexes on BP-1 were characterized by solid state NMR, FT-IR, elemental analysis, and metal digestion studies. Model, solution experiments were carried out to determine the site of electrophilic substitution on the pyridine ring of the pincer complexes and revealed substitution in both the *meta*- and *para*-position. The catalytic reactivity of immobilized (PNN)RuH(Cl)(CO) and (PONOP)RuH(Cl)(CO) on BP-1 was studied for the dehydrogenative coupling of alcohols to esters with the liberation of H_2. Moderate to good ester yields were realized with both immobilized systems without using the base required for the homogeneous reaction and also in the presence of KOH. The homogeneous model reactions required a base for alcohol formation. The amine functionality on BP-1 served as the base to generate the active pincer catalyst on the BP-1 surface. Both immobilized catalysts were recycled for multiple alcohol reaction cycles. Four-step control experiments were carried out using an alcohol and both immobilized systems. The results revealed the heterogeneity of the alcohol catalysis by both BP-1-Ru-PNN and BP-1-Ru-PONOP systems. This study has opened a new catalytic methodology for reactions where base is required for catalyst activation, by using a solid support with basic functionality.

Key words: Immobilization, Pincer complexes, Silica polyamine composite, Heterogeneous Catalysis, Ruthenium

1.1 Introduction

Immobilization of transition metal catalysts on a suitable solid surface has received significant attention in recent years. Though homogeneous systems provide remarkable activity and selectivity in catalytic reaction processes, they encounter very challenging issues in terms of separation of the products from the catalyst and low catalyst lifetime [1]. The heterogenization of homogeneous catalysts could help overcome these inherent problems and extend the use of relatively expensive catalysts in various chemical transformations [2]. Thus, immobilization chemistry constitutes a promising direction in the area of small molecule catalysis [3,4]. Immobilization facilitates easy product separation, recovery of relatively expensive catalysts by simple filtration, for reuse multiple catalytic cycles [3-11]. Though many synthetic techniques have been reported and utilized for immobilization of molecular organometallic catalysts on various support materials, the immobilization by covalent attachment of metal-ligand complexes on a suitable inorganic solid support appears to be the best way of recycling homogeneous catalysts [11-14].

We have focused on metal pincer complexes due to their wide range of applications in various catalytic reactions [15-17]. Though a wide variety of pincer ligands and their complexes are now accessible and have been shown to work as very effective catalysts, they are relatively expensive and their syntheses involves multiple complicated steps [18-20]. We and others have reported that direct immobilization of the preassembled pincer is the best method for immobilizing pincer ligands on surfaces [15, 21] There have been several reports recently on the immobilization of pincer metal complexes on various types of solid supports, including inorganic materials (alumina, silica), dendrimers, and functionalized organic polymers [22-24]. Silica materials have been shown to be very suitable solid supports for immobilization of organometallic pincer catalysts [25]. Pozo et al. reported the immobilization of (NHC)NN-pincer complexes on the mesoporous silica, MCM-41, by covalent binding of the pincers via pendant alkoxysilane groups [14]. Platinum and palladium NCN pincers, $[C_6H_3(2,6\text{-}CH_2NMe_2)_2]$ functionalized with para-ethynyl-groups were immobilized on azido-functionalized silica materials for C-C coupling reactions using “click” chemistry [26]. Palladium PCP pincer complexes were tethered to polymer and silica supports through amide or ether linkages and applied in the Heck reaction between iodobenzene and n-butylacrylate [27]. Brookhart et al. reported the immobilization of PCP and POCOP iridium pincer complexes for transfer dehydrogenation of alkanes on different types of solid supports using three approaches: 1) covalent attachment of phenoxide functionalized iridium pincers to a Merrifield's resin with the chlorobenzyl moieties; 2) covalent bonding of iridium pincers with a pendant alkoxysilane groups to silica; 3) adsorption of iridium pincers containing basic functional groups on γ-Al_2O_3 through a Lewis acid/Lewis base interaction [28]. Goldman et al. demonstrated the immobilization of bis-phosphinite-tert-butyl-irridium pincer complexes on γ-Al_2O_3 by two methods: 1) covalent attachment of trimethoxysilyl substituted iridium pincers with hydroxyl-functionalized Al_2O_3; 2) binding of *para*-functionalized POCOP iridium pincers to a coordinately-unsaturated surface site in Al_2O_3 [29]. The dihydride pincer complex [IrH_2(POCOP)] was also anchored on a mesoporous silica surface (SBA-15) by reaction of hydride with surface silanol groups and were then utilized as a heterogeneous catalyst for alkene hydrogenation reactions [30]. Pd(II)-SCS pincer complexes were covalently immobilized on porous silica, poly(norborene) and cross-linked Merrifield’s resin supports by C.W. Jones et al. and applied in the Heck reaction [31-32]. G. van Koten et al. reported the anchoring of PCP and SCS palladium pincer complexes on ordered mesoporous silica through a carbamate linkage between *para*-trialkoxysilane-functionalized palladium pincers and silica using a grafting process, and then utilized the supported catalysts in C-C bond formation reactions [25]. However, there is very limited information on heterogenization of PNN and PONOP ruthenium pincer complexes. In homogeneous reaction systems, PNN pincer complexes have been shown to act as excellent catalysts in many chemical transformations such as dehydrogenative coupling of alcohols to esters [33], hydrogenation of esters to alcohols [34], and amide formation from amines and alcohols [34]. Milstein showed that the catalytic activity of PNN pincer complexes requires a base to generate active catalyst complexes by deprotonation of the pincer arm [33-35]. More recently, an Fe-PNP complex has been shown to reduce CO_2 to formate at low pressures and also requires a base [36]. The PNP pincer, $Ir(H)_3(2,6\text{-}(iPr_2P)_2)NC_5H_3$, has been shown to be a highly efficient catalyst for the reduction of CO_2 to formate and requires a 10% aqueous KOH solution [37]. Similarly, the nickel PONOP pincer, $NiH(2,6\text{-}(iPr_2PO)_2)NC_5H_3)$, has been shown to be an effective hydrosilation catalyst in the presence of an aqueous base [18]. There are other reaction types, including aldol-type condensations with electrophiles, which require base using PCP and POCOP frameworks [38]. Thus, there is a large class of pincer-catalyzed reactions that require a base and would benefit from the elimination of the basic co-reagents by using a surface that could provide the required base.

In the present study, we utilize a silica polyamine composite, BP-1, which provides amine functionality on its surface that could act as a suitable base to generate the active PNN catalytic species upon binding or attachment of these complexes on the composite surface. The silica polyamine composites (SPC) were developed for the selective capture of metal and nonmetal ions and have been produced commercially for industrial applications in the recovery and removal of transition metals, precious metals, and mercury from diverse waste streams and mining leaches (Scheme 1) [39-42].

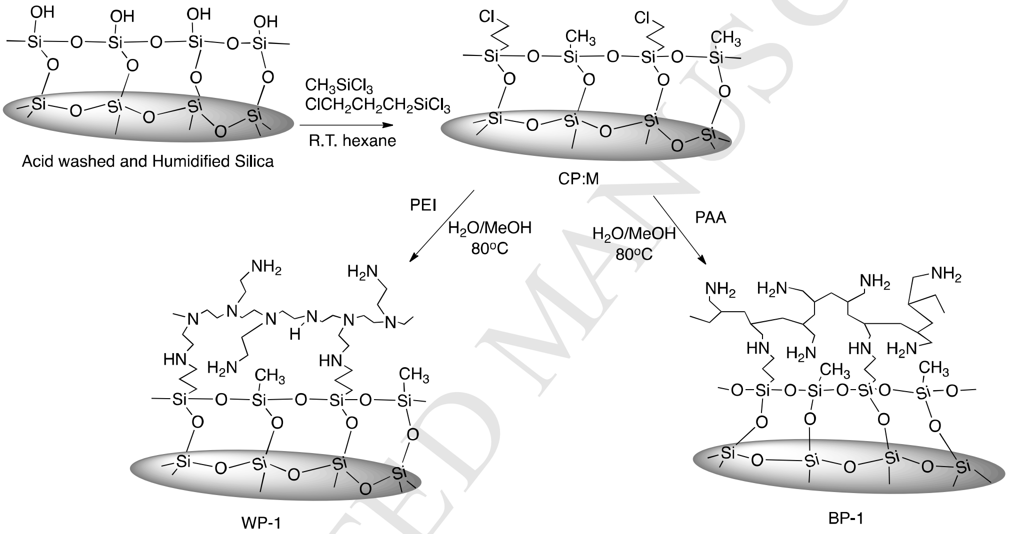

Scheme 1: Synthesis of silica polyamine composites

SPC are organic-inorganic hybrid materials with high porosity and the matrix rigidity of amorphous silica [40]. They have polyamine chelating agents covalently bound to the silane layers at multiple points that provide additional stability for the composites. In heterogeneous catalytic systems, the type and nature of the solid support is critical for obtaining the selectivity and performance of homogeneous catalysts [43-44]. Recently, we reported the application of rhodium, palladium and ruthenium salts immobilized on the SPC surface for selective hydrogenation of olefins and the selective oxidation of phenol to catechol [45]. In addition, various metal PONOP pincer complexes as well as a series of luminescent diimine ruthenium complexes have been successfully immobilized on SPC [7,15]. The surfaces of silica polyamine composites could control molecular access to the active sites of the catalysts in heterogeneous systems in a different way than simple oxide or polystyrene supports. For example, the unmodified amines offer the opportunity to act as base co-catalysts and permit tuning of the surface pH (Zeta potential).

This paper reports a study of immobilized PNN and PONOP pincer complexes of Ru on a silica polyamine composite, BP-1, in the dehydrogenative coupling of alcohols to give esters in the absence of a base and with KOH.

2. Experimental

2.1. General methods and materials

The SPC, referred to as BP-1 (1.5 mmol N/g), was synthesized using poly(allylamine) (MW = 11-15 Kg, Nitobo Buseki, Japan) (Scheme 1) [39-42]. The ligands, (PONOP) [2,6-bis(di-*tert*-butylphosphinito)pyridine] and PNN [{2-(di-*tert*-butylphosphinomethyl)-6-(di-ethylaminomethyl)}pyridine], and the pincer complexes (PONOP)RuH(Cl)(CO)and (PNN)RuH(Cl)(CO) were synthesized by previously reported procedures [33,46,47]. Solvents used were reagent grade. Tetrahydrofuran and 1,4-dioxane were distilled from benzophenone ketyl and methylene chloride and acetonitrile were distilled from calcium hydride. 2,6-Dihydroxy pyridine hydrochloride (Sigma Aldrich) and $(PPh_3)_3RuH(Cl)(CO)$ were purchased from Strem Chemicals, USA. Elemental analysis (C, H, N, P and Cl) were performed by Galbraith Laboratories, Inc, Knoxville, Tennessee, USA. Solid-state CPMAS and solution ^{13}C and ^{31}P NMR were obtained on a Varian NMR Systems 500 MHz spectrometer at 125 and 206 MHz respectively, with spinning speeds of 7-10KHz for the solid state experiments. ^{13}C and ^{31}P chemical shifts are reported relative to external tetramethylsilane and phosphoric acid respectively. Some solid state NMR spectra were recorded also on a Jeol ECZR 600 instrument operating at 600.17, 150,91 and 242.95 MHz for ^{1}H, ^{13}C and ^{31}P nuclei, respectively, respectively. The samples were packed in a cylindrical 3.2 mm diameter zirconia rotors rotor and spun at 20 kHz. All data were collected at ambient probe temperatures. All CPMAS experiments employed the Ramp-Amplitude Cross-Polarization pulse sequence (^{1}H 90° pulse = 3.05 μs, contact time = 1.5 ms, relaxation delay 0.2 s) with the Two Pulse Phase Modulation ^{1}H decoupling with an rf field of 75 kHz during the acquisition period. ^{1}H, ^{13}C and ^{31}P chemical shifts were referenced with the resonance of glycine (^{13}C methylene signal at 43.86 ppm) and 85% phosphoric acid (^{31}P signal at $\delta = 0$ ppm) as external standards. Infrared spectra were recorded as KBr pellets on a Thermo-Nicolet 633 FT-IR spectrometer. Loading of the metals on BP-1was determined by digesting the composite samples with a mixture of concentrated HCl and HNO_3 (6:1) [7] and the metal concentration in the digest was determined by Atomic Absorption (AA Spectrometer S Series, Thermo-electronic Corporation, USA). All reactions were carried out under a dry nitrogen or argon atmosphere using standard Schlenk techniques. In the catalytic reactions, the formation of esters and aldehydes from alcohols were determined by GC-MS with xylene as internal standard using an HP 5 column on an Agilent 6890N GC-MS system. Electron Microscopy images were obtained on a Hitachi H-7100. The results of all alcohol conversions were checked and verified by running the appropriate standard solutions of the corresponding alcohols by GC-MS. The results were also cross-checked by running the standard solutions of the corresponding esters as well. The reactions were monitored by GC-MS throughout the reaction period, which was determined by the times used by Milstein [33] for the related homogeneous reactions.

2.2 Immobilization of (PNN)RuH(Cl)(CO) on SPC-BP-1

(PNN)RuH(Cl)(CO) was immobilized on BP-1 by a two-step Mannich reaction [15]. 5g of BP-1 (containing 1.6 mmol N/g) was mixed with a reagent solution of 25 mL aqueous HCHO (38%, 345 mmol) and 0.5 mL glacial acetic acid (17.4M, 8.74 mmol) in a 250 mL flask equipped with an overhead stirrer. The suspension was stirred for 3–4 hours at room temperature yielding the surface-bound imine intermediate. The resulting composite was filtered and then washed several times with 95% ethanol, and then dried under vacuum overnight (yield: 5.19 g). 500 mg (0.885 mmol) of (PNN)RuH(Cl)(CO) [32] and 25 mL of distilled 1,4-dioxane were added to 5g of dried imine intermediate in a three-necked round bottom flask equipped with an overhead stirrer and a condenser. The mixture was degassed by applied vacuum (30 mmHg). The reaction mixture was refluxed overnight with stirring under N_2. The composite product was then filtered and washed four times with 1,4-dioxane, four times with acetone, and four times with CH_2Cl_2 and then dried overnight under high vacuum yielding 5.30 g of BP-1-(PNN)RuH(Cl)(CO) (**1**) product. Elemental analysis: C 12.74%, H 2.95%, N 2.84%, P 0.11%, Cl 2.30%. Solid-state CPMAS ^{13}C NMR, δ (ppm): 162.4 (pyridine), 33.5 (CH_2-polyamine), 56.7 (ethyl), 23.7 (*tert*-butyl), 15.1 (*tert*-butyl), 6.0 (Si-CH_3). CPMAS ^{31}P NMR, δ (ppm): 49.5. IR spectra (KBr pellet): 1948 cm-1 (s) (ν CO).

2.3 Immobilization of (PONOP)RuH(Cl)(CO) on SPC-BP-1 [15]

500 mg (0.885 mmol) of (PONOP)RuH(Cl)(CO) [46] and 25 mL of distilled THF were added to 5g of dried imine intermediate in a three-necked round bottom flask equipped with an overhead stirrer and a condenser. The mixture was degassed by applied vacuum (30 mmHg). The temperature of the mixture was raised to 70°C and the reaction mixture was refluxed overnight with stirring under N_2. The composite product was then filtered and washed four times with THF and four times with CH_2Cl_2 and then dried overnight under high vacuum yielding 5.34 g of BP-1(PONOP)RuH(Cl)(CO) (**2**) product. Elemental analysis: C 12.57 %, H 2.75%, N 2.42%, P 0.189%, Cl 0.27%. Solid-state CPMAS ^{13}C NMR, δ (ppm): 163.5 (pyridine), 48.5 (CH_2-polyamine), 33.8 (tert-butyl), 23.9 (*tert*-butyl), -5.9 (Si-CH_3). CPMAS ^{31}P NMR, δ (ppm): 58.1.IR spectra (KBr pellet): 1952 cm^{-1} (s) (ν CO).

2.4 Experimental procedure for model solution reaction between (PNN)RuH(Cl)(CO) and n-butyl amine

200 µL (2 mmol) of n-butyl amine was added to 200 µL (38%, 2 mmol) of HCHO solution. 20 µL (0.35 mmol) of glacial acetic acid (17.4 M) was added and the reaction mixture was stirred overnight at room temperature under N_2. The resulting imine intermediate was extracted with distilled CH_2Cl_2 and then anhydrous Na_2SO_4 was added to remove any trace H_2O. Solvent was then removed by rotary evaporation and the product was dried under high vacuum. 0.9 g (2 mmol) of (PNN)RuH(CO)Cl was combined with the dried imine intermediate in 10 mL distilled THF. The reaction was carried out at 66°C for 24 hours under N_2. Solvent was removed by rotary evaporation and the resulting product was washed with pentane and CH_2Cl_2.The product (PNN)RuH(Cl)(CO)-n-butyl amine (**3**) was purified by column chromatography eluting with the mixture of THF and hexane and then dried under high vacuum (yield: 0.72g, 1.26 mmol, 63%). ^{31}P NMR (Acetone-d_6): δ 89.79 (s), 90.36 (s), and 96.97 (s). ^{1}H NMR (Acetone-d_6) (three isomers) (δ ppm): 0.77 (t, $J_{H\text{-}H}$= 4.0 Hz, 3H, CH_3), 0.80 (t, $J_{H\text{-}H}$= 8.0 Hz, 3H, CH_3), δ 1.56 (t, $J_{H\text{-}H}$= 8.0 Hz, 3H, CH_3), δ 1.35 (t, $J_{H\text{-}H}$= 4.0 Hz, 3H, CH_3),δ 3.06 (t, $J_{H\text{-}H}$= 8.0 Hz, 3H, CH_3), 3.48 (m, 1H, N(C*H*HMe)$_2$), 3.31(m, 1H, N(C*H*HMe)$_2$), 1.22 (sextet, $J_{H\text{-}H}$= 8.1 Hz, 2H, CH_2), 1.74 (s, 18H, P-C(CH_3)$_3$), 5.05 (s, 2H, CH_2), 4.74 (s, br, 1H, N-*H*), 7.97 (s, 2H, *m*-pyridine, *para*-isomer),7.58 (dd, $J_{H\text{-}H}$= 4.0 Hz, 2H, pyridine, *meta*-isomer),1.42 (pent, $J_{H\text{-}H}$= 8.1 Hz, 2H, CH_2), 3.59 (d, $J_{H\text{-}H}$= 12.0 Hz, 2H, CH_2), -15.43 (d, J_{PH} = 28Hz, 1H, Ru-H). IR (ATR): 1931 cm^{-1} (s)(νCO), 2016 cm^{-1}(s) (νRu–H).

2.5 Experimental procedure for the deprotonation of (PNN)RuH(Cl)(CO)-n-butyl amine (3)

58 mg (0.1 mmol) of **3** was dissolved in THF (5mL). 11.2 mg (0.1 mmol) of KO^{t}Bu was added at -31°C and the mixture was stirred for 7 hours and then filtered. The volume of the deep-

red filtrate was reduced to 0.5 mL under vacuum and 5 mL pentane was added to precipitate the brown-red product. The product was then separated and washed three times with 2 mL pentane and dried under vacuum to yield (PNN-)RuH(CO)-n-butyl amine (**4**) (37 mg, 0.07 mmol, 69%). ^{31}P NMR (Acetone-d_6): δ 97.07 (s), 109.73 (s), and 109.78 (s). ^{1}H NMR (δ ppm) (Acetone-d_6) (three isomers): 0.78 (t, $J_{H\text{-}H}$= 4.0 Hz, 3H, CH_3), 3.07 (t, $J_{H\text{-}H}$= 4.0 Hz, 3H, CH_3), 4.17 (t, $J_{H\text{-}H}$= 8.0 Hz, 3H, CH_3), 1.22 (sextet, $J_{H\text{-}H}$= 8.0 Hz, 2H, CH_2), 0.78 (sextet, $J_{H\text{-}H}$= 4.0 Hz, 2H, CH_2),1.56 (m, 1H, N(C*H*HMe)$_2$), 2.12(m, 1H, N(C*H*HMe)$_2$),1.96 (s, 2H, CH_2),1.67(s, 2H, CH_2), 1.92 (vt, $J_{P\text{-}H}$ = 4.0 Hz, 9H, P-C(CH_3)$_3$), 1.93 (vt, $J_{P\text{-}H}$ = 4.0 Hz, 9H, P-C(CH_3)$_3$), 5.27 (s, 1H, = CHP), 5.27 (s, br, 1H, N-*H*),7.57 (dd, $J_{H\text{-}H}$= 8.0 Hz, 2H, pyridine, *meta*-isomer), -16.6 (d, $J_{P\text{-}H}$ = 16Hz, 1H, Ru-H). IR (ATR): 1929cm^{-1} (s) (ν CO), 2041cm^{-1}(m) (ν Ru–H).

2.6 Experimental procedure for the catalytic dehydrogenative coupling of 1-hexanol using 4 in the absence of solvent and with toluene

Complex **4** (0.01 mmol) was dissolved in 1-hexanol (10 mmol) in a small round bottom flask, equipped with a condenser. The solution was heated at 157°C under an argon flow for 56 hours. Conversion of 1-hexanol was measured at different time intervals by GC-MS. 1-Hexanol conversion to hexylhexanoate: 28% (after 2.5 hours of reaction), and 66% (after 56 hours of reaction). In the presence of solvent, the reaction was carried out following exactly same procedure except for the addition of 2 mL dried toluene. The results (1-hexanol conversion) are: 23 % (after 2.5 hours of reaction), and 59% (after 56 hours of reaction)

2.7 Experimental procedures for alcohol dehydrogenative coupling reactions catalyzed by 1 in the absence of a base and with KOH

200 mg of **1** (0.007 mmol) was placed in a small round-bottom flask. 21 mmol of alcohol was added. In the case of 1-hexanol, 400 mg (0.014 mmol) of **1** was added to 35 mmol of alcohol. An applied vacuum degassed the mixture. The mixture was then heated with slow stirring under an inert atmosphere of argon. The reaction mixture was cooled to room temperature and the composite catalyst was separated by filtration. The resulting liquid product mixture was analyzed by GC-MS. Total alcohol conversion and reaction conditions for each alcohol used are summarized in Table 1.

2.8 Experimental procedures for catalytic dehydrogenative coupling of alcohols to esters by (PONOP)RuH(Cl)(CO) in solution

12 mg of (PONOP)RuH(Cl)(CO) (0.02 mmol) was placed in a small round-bottom flask. 20 mmol of alcohol was added. The mixture was degassed by an applied vacuum and then heated with slow stirring under at inert atmosphere of argon. The reaction mixture was cooled to room temperature. The liquid product mixture was analyzed by GC-MS. Total alcohol conversion and reaction conditions for each alcohol are summarized in Table 2.

2.9 Experimental procedures for dehydrogenative coupling of alcohols catalyzed by 2 in the absence of base and with KOH

200 mg of **2** (0.007 mmol catalyst on BP-1) was placed in a small round-bottom flask. 21 mmol of alcohol was added. In the case of 1-hexanol, 400 mg of **2** was added into 35 mmol of alcohol. The mixture was degassed by applied vacuum. The mixture was then heated with slow stirring under an atmosphere of argon. The reaction mixture was cooled to room temperature and the composite catalyst was separated by filtration. The resulting liquid product mixture was analyzed by GC-MS using an HP 5 column on an Agilent 6890N GC-MS system. Total alcohol conversion and reaction conditions for each alcohol are summarized in Table 3.

2.10 Reaction protocols for 1-heptanol catalysis with 1 in dichlorobenzene in the absence of base and with KOH

200 mg **1** (0.007 mmol) and 21 mmol of 1-heptanol were mixed in a small round-bottom flask. 2 mL dichlorobenzene was added. The mixture was degassed by applied vacuum. The mixture was then refluxed with slow stirring under an inert atmosphere of argon for 48 hours. The reaction mixture was cooled to room temperature. The liquid product mixture and catalyst were separated by filtration. Formation of heptylheptanoate and 1-heptanal was determined by GC-MS. Total 1-heptanol conversion: 33%. heptyl heptanoate: 32%. 1-heptanal: 1%. Exactly the same procedure was followed for the reaction with base where 0.007 mmol of KOH was added to the reactant mixture. The results were: heptylheptanoate: 38%. 1-heptanal: 2%

2.11 Reaction protocols for 1-heptanol catalysis with 2 in dichlorobenzene in the absence of a base and with KOH

200 mg **2** (0.007 mmol Ru-PONOP on BP-1) and 21 mmol of 1-heptanol were mixed in a small round-bottom flask. 2 mL of 1,2-dichlorobenzene was added. The mixture was degassed by applied vacuum. The mixture was then refluxed with slow stirring under an atmosphere of argon for 48 hours. The reaction mixture was cooled to room temperature. The liquid product mixture and catalyst were separated by filtration. The formation of heptylheptanoate and 1-heptanal was determined GC-MS. Total 1-heptanol conversion: 30%, heptylheptanoate 29% and 1-heptanal 1%. The same procedure was followed for the reaction with base where 0.007 mmol of KOH was added to the reactant mixture. 1-Hepanol total conversion were: 36%, heptyl-heptanoate 33 % and 1-heptanal 3%)

2.12 Experimental procedure for the cycle studies of alcohol dehydrogenative coupling with 1.

2.12.1 Reaction protocols for conversion of alcohols to the corresponding esters and hydrogen by the solid-liquid method (Slow stirring the mixture of catalyst and alcohol).

In the solid-liquid method, alcohols and BP-1-Ru-PNN (**1**) mixtures were stirred slowly with a small magnetic stir bar under an atmosphere of argon. Temperature and other reaction conditions were described in Table 1 & 4. When the reaction was stopped, the composite catalyst and liquid product mixture was separated by filtration and then the catalyst was washed with acetone, toluene, and CH_2Cl_2 and dried under high vacuum. The liquid-product mixtures were analyzed by GC-MS. The dried **1** was used for the next cycle and the overall procedure was repeated. Yields and conversion of alcohols to corresponding esters in each of the successive cycles are given in Table 4.

2.12.2 Reaction protocols for the dehydrogenative coupling of alcohols using the solid-vapor method (passing the alcohol vapor over the catalyst bed).

In the solid-vapor method, the required amount of composite catalyst (as mentioned in Table 1 and section 2.7) was placed on a glass frit fitted with 14/20 male and female ground glass joint. The frit was then equipped with a small round bottom flask on the bottom containing the appropriate amount of alcohol (section 2.7). A water condenser was placed on the top of the frit. The whole system was then degassed by applied vacuum. Alcohol vapor was created by heating the round bottom flask. The alcohol vapor condensed after passing through catalyst bed, and then back to the round bottom flask, through the catalyst bed. After the reaction was over, the system was cooled to room temperature and the apparatus was disassembled. The liquid product mixture was collected and then analyzed by GC-MS. The composite catalyst was washed with acetone, toluene, and CH_2Cl_2 and dried under high vacuum. The dried composite catalyst was used for next cycle and the overall procedure was repeated. Yields and conversion of alcohols to corresponding esters are given in the Table 4-5. Solid-state CPMAS ^{13}C NMR data and FT-IR data on BP-1-Ru-PNN (**1**) after catalysis are given in Table 1S. The results of elemental analysis and metal digestion study on BP-1-Ru-PNN (**1**) after catalysis are shown in Table 2S.

2.13 Experimental procedures for cycle study in alcohol dehydrogenative coupling with 2

The procedures for cycle study in alcohol dehydrogenation reaction with **2** were the same as those described in the section 2.12. Reaction conditions and catalyst to alcohol ratios were mentioned in the section 2.9 and Table 3. Yields and conversion of alcohols to corresponding esters are given in the Table 5. Solid-state ^{13}C CPMAS NMR data and FT-IR data on BP-1-Ru-PONOP after catalysis are given in Table 3S. The results of elemental analysis and metal digestion study on BP-1-Ru-PONOP after catalysis are shown in Table 4S.

2.14.1 Experimental procedure for the control experiments with 1-hexanol and 1 in the absence of base

400 mg of **1** (0.014 mmol) was placed in a small round-bottom flask. 35 mmol of 1-hexanol was added. The flask was equipped with a condenser. The mixture was degassed by applied vacuum. Then the following steps were done:

Step 1: The mixture of 1-hexanol and **1** was stirred slowly for 4-5 hours under an atmosphere of argon. 100µL of the resultant liquid was collected and diluted with toluene and analyzed by GC-MS. Yield (1-hexanol conversion): 0%.

Step 2: The mixture was stirred and heated overnight (about 15-16 hours) at 157°C under the flow of argon. The mixture was then cooled to room temperature. 100µL of the resultant liquid was taken and diluted with toluene and the analyzed by GC-MS. Yield (1-hexanol conversion): 30%.

Step 3: The resultant mixture of 1-hexanol and **1** from step 2 was stirred with heating at 157°C under the flow of argon for an additional 4 hours. The reaction mixture was cooled to room temperature and the liquid product mixture was separated from the solid catalyst. 100µL of the liquid mixture was diluted with toluene and analyzed by GC-MS. Yield (1-hexanol conversion): 4%.

Step 4: The resultant liquid product mixture obtained from step 3 was separated from the catalyst and placed in a small round bottom flask equipped with a condenser and degassed by applied vacuum. In the absence of the catalyst, it was stirred and heated at 157°C under an atmosphere of argon overnight (about 15-16 hours). It was then cooled to room temperature and analyzed by GC-MS. Yield (1-hexanol conversion): 2-3%.

2.14.2 Experimental procedure for the control experiment with 1-hexanol and 1 in the presence of KOH

400 mg of **1** (0.014 mmol) and 0.014 mmol of KOH were mixed in a small round-bottom flask. 35 mmol of 1-hexanol was added. The mixture was degassed by applied vacuum. Then steps 1 to 4 as described in section 2.14.1 were repeated. Conversion of 1-hexanol in each of the steps was determined by using GC-MS. The results are as follows: Step 1: No conversion; Step 2: 36% ; Step 3: 7% and Step 4: 3%.

2.15.1 Experimental procedure for the control experiment between 1-hexanol and 2 in the absence of a base

400 mg of **2** (0.014 mmol Ru-PONOP on BP-1) and 35 mmol of 1-hexanol were mixed in a small round-bottom flask. The mixture was degassed by applied vacuum. Then the reactions were conducted following steps 1 to 4 described in section 2.14.1. Conversion of 1-hexanol to hexyl hexanoate in each of the steps was determined by using GC-MS. Yields: Step1: No conversion; Step 2: 25% ; Step 3: 4% and Step 4: 2%

2.15.2 Experimental procedure for the control experiment with 1-hexanol and 2 in the presence of KOH

400 mg of Ru-PONOP-BP-1 (**2**) (0.014 mmol Ru-PONOP on BP-1) and 0.014 mmol of KOH were mixed in a small round-bottom flask. 35 mmol of 1-Hexanol was added. The mixture was degassed by applied vacuum. Then the reactions were carried out following steps 1 to 4 described in section 2.14.1. Conversion of 1-hexanol to hexyl hexanoate in each of the steps was

determined by using GC-MS. Yields: Step1: No conversion; Step 2: 29%; Step 3: 6% and Step 4: 3%

3. Results and discussion

3.1 Immobilization and catalytic study with (PNN)RuH(Cl)(CO) on BP-1 (1)

(PNN)RuH(Cl)(CO) pincer complex was immobilized on the BP-1 surfaces following a two-step Mannich reaction reported recently for (PONOP)RuH(Cl)(CO) [15]. In the case of the symmetrical (PONOP)RuH(Cl)(CO) two regio-isomers are possible and this was verified by model studies in solution (Scheme 2). In the case of (PNN)RuH(Cl)(CO) three regio-isomers are possible but solid state data shows resonances too broad to resolve them and so solution model studies were undertaken to confirm this (*vide infra) (*Scheme 2).

The loading of the complex on BP-1 was confirmed by solid-state NMR, FT-IR, elemental analysis, and metal digestion data. Solid-state CPMAS ^{13}C spectra of the tethered complex showed resonances at δ 162.4 ppm for the pyridine carbons, 23.7 ppm for *tert*-butyl carbons, and 56.7 ppm for the carbons from the ethyl groups in the complex, which were similar to the resonances observed for the complex in solution [33]. In addition CPMAS ^{31}P NMR spectra displayed a single resonance at δ 49.5 ppm indicating the successful loading of the complex on BP-1 surfaces.

The imine-functionalized BP-1 intermediate showed a characteristic $\nu_{C=N}$ at ~ 1662 cm^{-1} which was not observed in the spectra of pristine BP-1. The presence of an amine stretch at 1635 cm^{-1} shows that not all the amine groups have been converted to imine groups (Scheme 2) (15). Upon combination with the corresponding pincer complexes this resonance should have disappeared if all imine groups on BP-1 interact with the pincers. In fact, a small decrease in intensity of this resonance was realized after the metal pincer complexes were attached to the

BP-1, which indicates the relatively low loading of the complexes on the composite surface. The carbonyl group in the (PNN)RuH(CO)(Cl) complex showed ν CO stretch at 1948 cm^{-1} in the FT-IR spectra evidence that the heterogenization of the complex on the composite, BP-1. Upon immobilization, a large shift in CO frequency of the complex was realized in comparison to the solution phase (1901 cm^{-1}) [33], which is likely due to changes in electronic environment and ring substitution of the complex on BP-1 [15]. Similar shifts of the CO frequency were also noticed in our previous study with the (PONOP)RuH(Cl)(CO) pincer complex on BP-1 [15].

The FT-IR spectra of the product, (PNN)RuH(Cl)(CO)-n-butyl amine (**3**), obtained from the model solution study between (PNN)RuH(Cl)(CO) and n-butyl amine, displayed a CO stretching frequency at 1931 cm^{-1} (*vide* infra)indicating that attachment of an alkyl chain in the pyridine ring of the complex dramatically affects the electronic environment of the complex, resulting in the large shift of the CO stretching frequency [49]. Loading of the complex was found to be 0.038 mmol/g BP-1 based on the metal digestion study. The % P analysis from elemental analysis data provided the loading of the complex, 0.035 mmol/g BP-1, in reasonable agreement with the results of the metal digestion study, confirming the presence of (PNN)RuH(Cl)(CO) on BP-1.

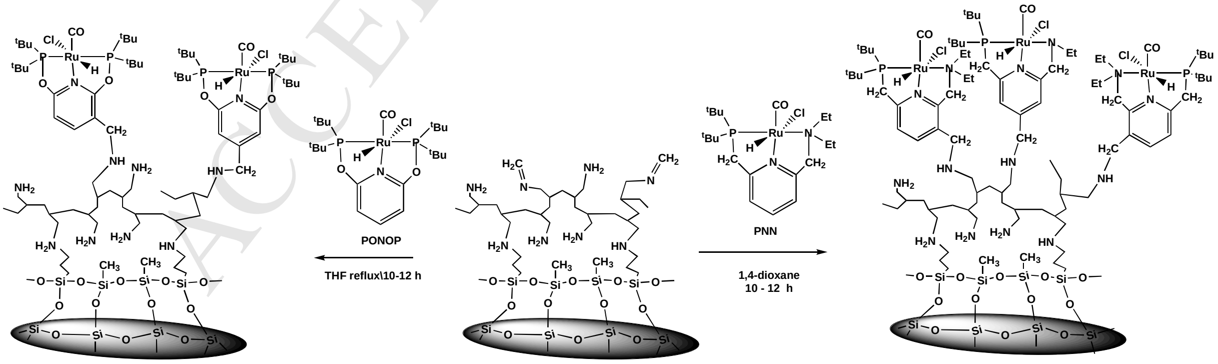

Scheme 2: Immobilization of (PNN)RuH(Cl)(CO) and (PONOP)RuH(Cl)(CO) on BP-1 [15].

The impact of immobilization of the PNN and PONOP metal pincer complexes on surface area, structure and porosity of the silica polyamine composite, BP-1 was assumed to be very negligible particularly considering the extent of loading of the pincers (~0.04 mmol complex /g BP-1) [15]. Our previous study on covalent tethering of luminescent Ru complexes on BP-1 with similar loading did not show any measurable change of the porosity and structure of the composite surface [7,15].

The catalytic reactivity of **1** in the dehydrogenative coupling of alcohols to the corresponding esters with the liberation hydrogen was then investigated. The reactions were carried out with three primary alcohol systems: 1-hexanol, 1-heptanol, and benzyl alcohol, and a secondary alcohol, 2-octanol. All reactions using **1** were conducted in the absence of a base and then with the addition of 1 eq. KOH. The results were compared with the homogeneous systems reported by Milstein et al. [33]. The catalyst-to-alcohol ratio used in the reaction system was 0.007:21 (equivalent to 0.01:30) except in the case of 1-hexanol, where 0.014 mmol of catalyst was used with 35 mmol of alcohol (equivalent ratio, 0.02:50) (Table 1). In all reactions a large excess alcohol was used to accommodate the solid catalyst, in comparison to the catalyst-to-alcohol ratios previously reported for the homogeneous reaction system (0.1 mmol catalyst : 10 mmol alcohol) [33]. Alcohol catalysis with **1** produced the corresponding esters and hydrogen. However, in some cases, aldehydes were also formed along with major ester products (Table 1).

Reaction of 1-hexanol with **1** with 0.04 mol% catalyst at 157°C for 56 hours resulted in the formation of hexylhexanoate, hydrogen, and a trace of 1-hexanal with an overall conversion of 50%. When KOH (equivalent to Ru-PNN) was used, ester yield increased to 62% (Table 1). Homogeneous reaction with the 0.1 mol% of the same catalyst investigated by Milstein et al.

reported the conversion at 91 to 95% after 24 hours in the presence of KOH, following similar reaction conditions [33].

Heterogeneous catalysis of 1-heptanol with 0.03 mol% **1** showed a total of 52% conversion with 51% of heptylheptanoate and 1% 1-heptanal when the reaction was carried out at 176°C for 48 hours under argon. However, with KOH (1 equivalent to Ru-PNN), conversion improved to 64% (62 % heptylheptanoate and 2% 1-heptanal) (Table 1). Similarly, heating a mixture of benzyl alcohol with 0.03 mol% **1** at 178°C for 60 hours, gave benzylbenzoate and benzaldehyde in 38% and 10 % yields (Table 1). With the addition of KOH (equivalent to Ru) total conversion increased to 55%, with 43% benzylbenzoate and 12% benzaldehyde whereas the homogeneous reaction system with 0.1 mol% Ru-PNN provided a 93% yield with only 1% benzaldeyde [33].

Table 1: Conversion of alcohol to corresponding esters and hydrogen with immobilized (PNN)RuH(Cl)(CO) on BP-1 (**1**) in the absence of a base and with KOH

Alcohol	Base (mmol)	Catalyst/ Alcohol ratio (mmol)	Reaction Temp (°C)	Reaction Time (Hours)	Total alcohol conversion (%)	Turnover frequency (Hour $^{-1}$)
1-Hexanol	-	0.02/50	157	56	50 (49% Hexyl hexanoate and 0.5% 1-Hexanal)	22
	0.02	0.02/50	157	56	62 (61% Hexyl hexanoate and 0.8% 1-Hexanal)	28
1-Heptanol	-	0.01/30	176	48	52 (51% Heptyl heptanoate and 1% 1-Heptanal)	33
	0.01	0.01/30	176	48	64 (62% Heptyl heptanoate and 2% 1-Heptanal)	40
Benzyl alcohol	-	0.01/30	178	60	48 (38% Benzyl benzoate and 10% Benzaldehyde)	24
	0.01	0.01/30	178	60	55 (43% Benzyl benzoate and 12% Benzaldehyde)	28
2-octanol	-	0.01/30	178	48	53% 2-octanone	33
	0.01	0.01/30	178	48	58% 2-octanone	36

The percentage of benzaldehyde was observed to be a bit higher with **1** in comparison with the homogeneous reactions [33]. The secondary alcohol 2-octanol, yielded only 2-

octanone, and hydrogen with a conversion of 53% when treated with 0.03 mol% **1** at 178°C for 48 hours under argon. When 1 eq. KOH was used, the 2-octanone the yield increased to 58%. 2-Octanone was also the only product formed in the homogeneous reaction [33].

No reaction occurred in the homogeneous reaction between (PNN)RuH(Cl)(CO) and alcohols when there was no base present [33]. Catalysis with **1** produced esters and H_2 in the absence of a base as well as with KOH (Table 1). However, a longer reaction period was required and lower yields were realized in all cases with **1** in comparison to the homogeneous reactions. The homogeneous systems used 0.1mole % catalyst, whereas in the present study, 0.03 mole % of immobilized catalyst was utilized and a larger excess of alcohol was used in each case. Lower catalyst concentration would definitely affect the alcohol conversion rate in the heterogeneous systems reported here.

The moderate to good yields of esters and H_2 reported herein in the absence of KOH provides evidence that the amine functionality on the BP-1 surface served as the required base to deprotonate the pincer arm (-CH_2 group) of (PNN)RuH(Cl)(CO) and formed deprotonated or dearomatized active catalyst, [(PNN)RuH(CO)] on BP-1 (Scheme 3). Though an amine is a weaker base than KOH, the higher temperature and surface confinement make the deprotonation more favorable [48]. Both the original and dearomatized Ru-PNN complexes could be present on BP-1 after immobilization. We are unable to quantify the approximate proportion of deprotonated/dearomatized active catalyst relative to the original complex [(PNN)RuH(Cl)(CO)] present on BP-1 after immobilization. FT-IR and solid-state NMR spectra did not provide much information about the differences in the resonances between the two forms of the complexes on BP-1.

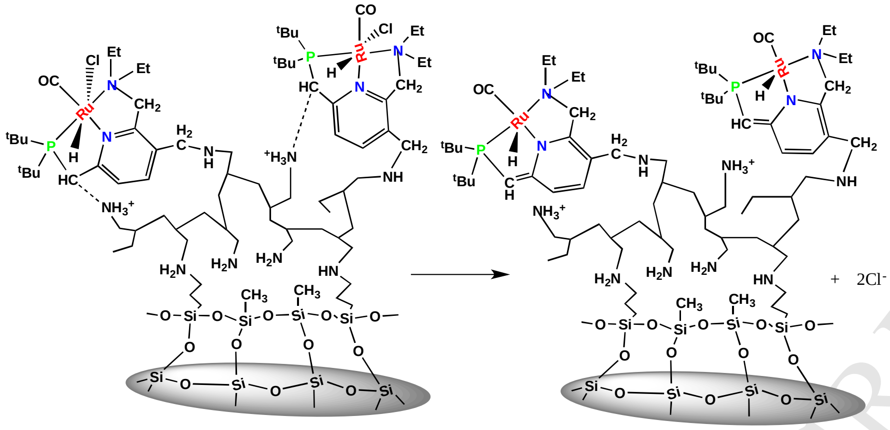

Scheme 3: Deprotonation of the pincer arm (-CH_2 group) in (PNN)RuH(Cl)(CO) by amines on the BP-1 surface

However, better conversion of alcohols was observed in all four cases when the catalytic reactions were conducted in the presence of KOH, which indicates that all loaded or immobilized Ru-PNN molecules might not be deprotonated by the surface amines. Application of KOH likely results in the generation of more dearomatized [(PNN)RuH(CO)] complex on BP-1, and thus enhanced the catalytic conversion of alcohols to esters.

3.2 Model solution reaction between (PNN)RuH(Cl)(CO) and n-butyl amine and a catalytic study with the deprotonated form of the product

Determination of the actual position of the substitution in the pyridine moiety of (PNN)RuH(Cl)(CO) upon immobilization on the BP-1 surface was relatively difficult due to the poor resolution of the solid-state NMR data. Substitution at the *meta*-position would be preferable on electronic grounds, while *para*-substitution might be expected on steric grounds. To clarify this point, two-step model solution reactions was carried out between (PNN)RuH(Cl)(CO) and n-butyl amine following a previously reported procedure [15]. Analyses of the product with ^{31}P NMR spectroscopy showed three resonances at δ 89.97, 90.36, and 96.97

ppm (Figure 1), which indicates the formation of the mixture of three isomers. The resonance at δ 96.97 ppm could be for the *para*-isomer. Two *meta*-isomers showed resonances at δ 89.97 and 90.36 ppm with almost equal integration. The relative intensity of the resonances suggested the formation of about 84% *meta*-isomers (42% each) and 16% *para*-isomer. The FT-IR spectrum of the isomeric product mixture showed a carbonyl stretch at 1931 cm^{-1}, which was higher by 30 cm^{-1} than the original complex (1901cm^{-1}) [33]. This indicates that the CO stretching frequency for the (PNN)RuH(Cl)(CO) is very sensitive to substitution on the pyridine ring [15]. There is ample evidence in the literature that substituents on the pincer ring can significantly affect infrared stretching frequencies on pincer catalysts [49]. These results rationalized the appearance of the CO stretching frequency at 1948 cm^{-1} upon immobilization of (PNN)RuH(Cl)(CO) on BP-1, which was much higher than that of the original complex (1901cm^{-1}) before loading. The environment on the surface must also affect the CO stretching frequency in the FT-IR in addition to the observed substituent effects [15].

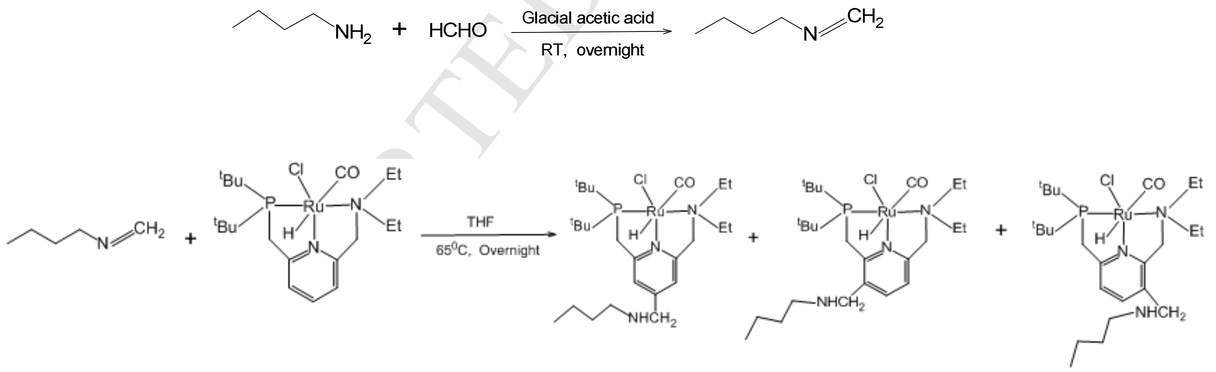

Ru-PNN-n-butyl amine (*para*-isomer, **3i**)

Ru-PNN-n-butyl amine (*meta*-isomers, **3ii, 3iii**)

Overall yield: 63%

Scheme 4: Model solution reaction between (PNN)RuH(Cl)(CO) and n-butylamine

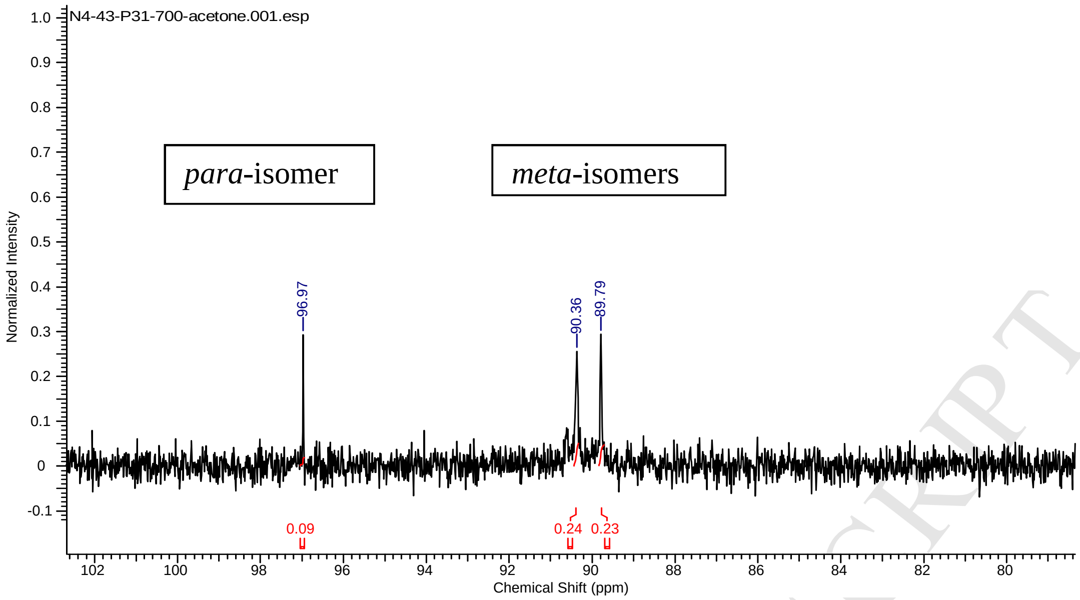

Figure 1: ^{31}P NMR spectrum of the isomers (**3)** in CD_2Cl_2 formed from the reaction of n-butylamine with (PNN)RuH(Cl)(CO)

Chemical treatment of complex **3** with KO^{t}Bu following the procedure reported for the original pincer complex, (PNN)RuH(Cl)(CO) [33], produced the deprotonated active pincer complex (PNN-)RuH(CO)-n-butyl amine (**4)** (Scheme 5). ^{31}P NMR showed three resonances at δ 97.07 (s), 109.73 (s), and 109.78 (s), which indicated the deprotonation of all three isomers of **4** (Figure 2). The resonance at δ 97.07 is assigned to a deprotonated *para*-isomer. The other two overlapping resonances at δ 109.73 (s) and 109.78 (s), are assigned to two *meta*-isomers (Figure 2). FT-IR spectra of the deprotonated product showed the CO stretching frequency at 1929 cm^{-1}, which was not much different than before deprotonation (1931 cm^{-1}). Very similar carbonyl stretching frequency differences were observed with (PNN)RuH(Cl)(CO) before (1901 cm-1) and after deprotonation (1889 cm^{-1}) reported by David Milstein et al. [33].

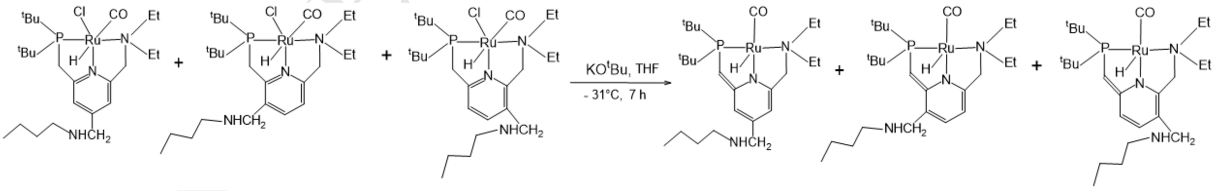

1 (*para*-isomer) (**4i)**

4 (*meta*-isomers) (**4ii, 4iii**)

Overall yield: 69%

Scheme 5: Formation of dearomatized active catalyst (PNN-)RuH(CO)-n-butyl amine (**4**) by reaction of (PNN)RuH(Cl)(CO)-n-butyl amine (**3**) with KO^{t}Bu

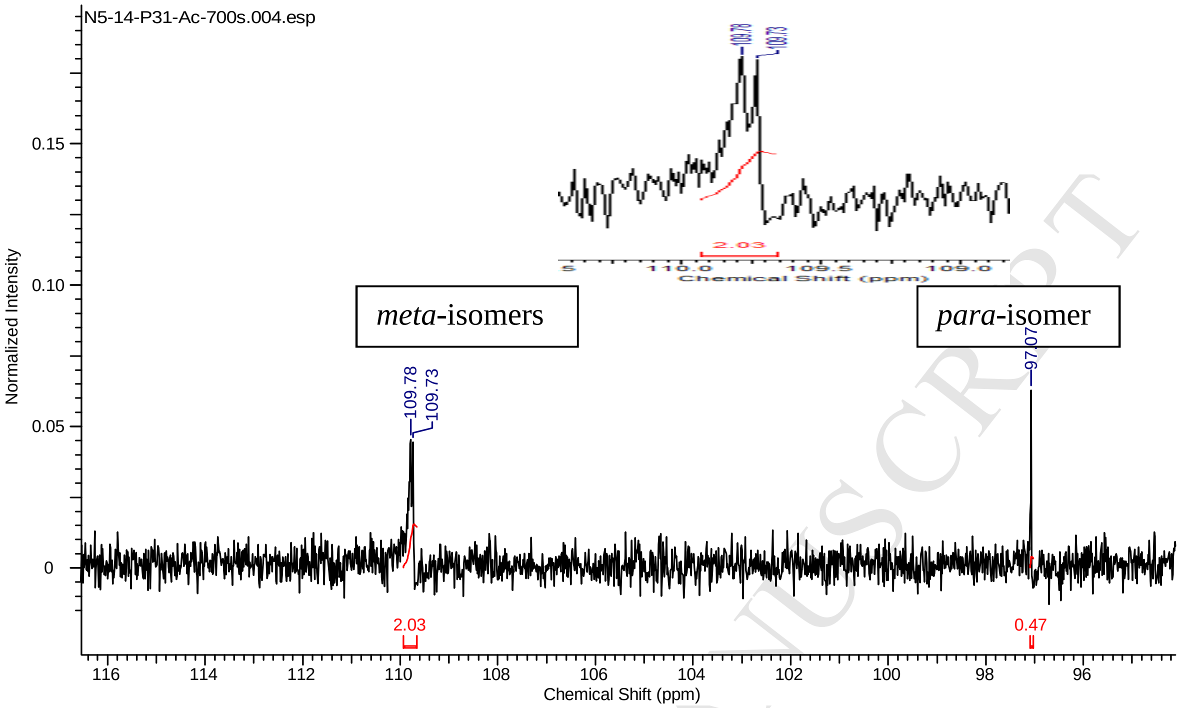

Figure 2: ^{31}P NMR spectrum of the isomeric products (**4**) in CD_2Cl_2 formed from the deprotonation of (PNN)RuH(Cl)(CO)-n-butylamine (**3**) by KO^{t}Bu

1-Hexanol catalysis with 0.1 mol% of (PNN-)RuH(CO)-n-butyl amine (**4**) at 157°C under an argon flow yielded only 28% product after 2.5 hours. However, the dearomatized complex reported by Milstein et. al (PNN)RuH(CO), under similar reaction conditions gave 91% conversion after 2.5 hours [33]. When the reaction was continued for 56 hours, total conversion was found to be 66% with 65% hexyl hexanoate and 0.5% 1-hexanal. In the presence of toluene, the reaction in **4** yielded only 23% after 2.5 hours. The same reaction with 0.1 mol% dearomatized (PNN)RuH(CO) provided 99% conversion of 1-hexanol to hexyl hexanoate in toluene after 6 hours [33]. These results indicate that introduction of an n-butyl amine substituent on the pyridine ring of (PNN)RuH(Cl)(CO) decreases its catalytic reactivity. This decrease could be due to steric hindrances of the long n-butyl chain or electronic effects from the increased electron donating ability amino-alkyl on the coordination equilibria between the alcohol and the dearomatized complex. There are a few examples in the literature on how the substituents in the pincer complex structure affect their catalytic reactivity [36, 50].

3.3 Catalytic study of (PONOP)RuH(Cl)(CO) in dehydrogenative coupling of alcohols to esters and hydrogen

The (PONOP)RuH(Cl)(CO) pincer complex was immobilized on BP-1 following a previously reported procedure (Scheme 2) [15]. Though many PONOP metal complexes have been reported in the literature, to date, there have been no reports of catalysis with the (PONOP)RuH(Cl)(CO) pincer complex system [48,50,51]. Based on the solution behavior of this complex it was suggested that it might not be stable enough under catalytic reaction conditions [46]. However, its analogue, (PNN)RuH(Cl)(CO), has shown catalytic reactivity in a variety of chemical transformations [33,52-59]. In light of this, we decided to investigate the catalytic reactivity of (PONOP)RuH(Cl)(CO) in the dehydrogenative coupling of alcohols under both homogeneous and heterogeneous conditions.

In both the homogeneous reaction and immobilized on BP-1 the (PONOP)RuH(Cl)(CO) displayed catalytic reactivity toward the dehydrogenative coupling of alcohols moderate yields [60]. The results of alcohol catalysis by (PONOP)RuH(Cl)(CO) are presented in Tables 2 and 3. No alcohol conversion was realized in the absence of a base irrespective of the alcohol used (Table 2). However, when the reactions were conducted in the presence of KOH equivalent to R(PONOP)RuH(Cl)(CO), all alcohols produced the corresponding esters and hydrogen, which suggested that a base is required to generate an active catalyst from (PONOP)RuH(Cl)(CO) in alcohol dehydrogenative coupling reactions. The chemical reaction of 1-hexanol with 0.1 mol% (PONOP)RuH(Cl)(CO) for 36 hours at 157°C under argon yielded 61% hexylhexanoate. Similarly, 1-heptanol was catalyzed by 0.1 mol% (PONOP)RuH(Cl)(CO) for 24 hours at 176°C under argon and produced 67% heptylheptanoate, 2% 1-heptanal, and hydrogen with a turnover frequency of 58 h^{-1}. Benzyl alcohol reacting with Ru-PONOP at 178°C under argon, with the same alcohol-to-catalyst ratio resulted in the formation of benzylbenzoate, benzaldehyde, and hydrogen with an overall conversion of 66%. 2-Octanol yielded only 2-octanone in 65% yield under the same conditions.

Table 2: Dehydrogenative coupling of alcohols (PONOP)RuH(Cl)(CO) in solution in the absence of a base and with KOH.

Alcohol	Base (mmol)	Catalyst/ Alcohol ratio (mmol)	Reaction Temp (°C)	Reaction Time (Hours)	Total alcohol conversion (%)	Turnover frequency (Hour $^{-1}$)
1-Hexanol	-	0.01/10	157	36	0	-
	0.01	0.01/10	157	36	61 (60% Hexyl hexanoate and 0.5% 1-Hexanal)	17
1-Heptanol	-	0.01/10	176	24	0	-
	0.01	0.01/10	176	24	69 (67% Heptyl heptanoate and 2% 1-Heptanal)	28
Benzyl alcohol	-	0.01/10	178	24	0	-
	0.01	0.01/10	178	24	66 (62% Benzyl benzoate and 4% Benzaldehyde)	27
2-octanol	-	0.01/10	178	24	0	-
	0.01	0.01/10	178	24	65% 2-octanone	28

1-Heptanol catalysis with 0.01 mol% Ru-PONOP-n-butyl amine (obtained from the reaction between (PONOP)RuH(Cl)(CO) and n-butyl amine [15]), in the presence of KOH (equivalent to Ru) at 176°C under argon yielded 42% conversion of 1-heptanol after 24 hours, and continuation of the reaction up to 48 hours resulted in 54% 1-heptanol conversion to heptylheptanoate. The introduction of an alkyl substituent in the structure of Ru-PONOP decreased its catalytic activity, as for the PNN case [50]. A similar reaction between Ru-PONOP-n-butyl amine and 1-heptanol in the absence of KOH did not result in the formation of any esters indicating that amine functionality in the n-butyl substituent was not involved in the catalytic reaction.

The catalytic study of (PONOP)RuH(Cl)(CO) on BP-1 (**2**) in dehydrogenative coupling showed similar results to the homogeneous reactions albeit with lower yields. When 1-hexanol, was treated with **2 (**0.02 mol%) at 157°C for 56 hours under argon, only 26% of hexylhexanoate was observed. Addition 1 eq. of KOH increased the conversion to 36%. Repetition of the reaction with more catalyst (0.04 mol%) improved the alcohol conversion to 43% without base and 47% when KOH was used (Table 3). Other alcohols gave similar yields with catalyst **2**. 1-Heptanol treated with 0.03 mol% **2** at 176°C for 48 hours under argon, gave an overall conversion of 55% with a turnover frequency of 46 h^{-1} (Table 3). With KOH (1 equivalent to Ru), 60% conversion of 1-heptanol was observed. Benzyl alcohol reacted in a similar way, with **2**. Using a 1:30 ratio of catalyst to alcohol at 178°C under argon for 60 hours gave 49% conversion with 38% benzyl benzoate, 11% benzaldehyde, and H_2. Like the 1-heptanol catalysis, an increase in reaction yield was realized upon addition of 1 eq. of KOH (Table 3). 2-Octanol gave only 2-octanone and H_2 in 48% yield upon reaction with 0.03 mol% of **2** at 175°C for 48 hours, with a turnover frequency of 33 h^{-1}. The addition of 1 eq. KOH increased the ketone yield to 54%.

Table 3: Dehydrogenative Coupling with **2** in the absence of base and with KOH

Alcohol	Base (mmol)	Catalyst/ Alcohol ratio (mmol)	Reaction Temp (°C)	Reaction Time (Hours)	Total alcohol conversion (%)	Turnover frequency (Hour $^{-1}$)
1-Hexanol	-	0.02/50	157	56	43 (42% Hexyl hexanoate and 0.6% 1-Hexanal)	19
	0.01	0.02/50	157	56	47 (46% Hexyl hexanoate and 0.7% 1-Hexanal)	21
1-Heptanol	-	0.01/30	176	48	55 (52% Heptyl heptanoate and 3% 1-Heptanal)	34
	0.01	0.01/30	176	48	60 (56% Heptyl heptanoate and 4% 1-Heptanal)	38
Benzyl alcohol	-	0.01/30	178	60	49 (38% Benzyl benzoate and 11% Benzaldehyde)	25
	0.01	0.01/30	178	60	56 (42% Benzyl benzoate and 14% Benzaldehyde)	28
2-octanol	-	0.01/30	178	48	48% 2-octanone	30
	0.01	0.01/30	178	48	54% 2-octanone	34

The observed catalysis with (PONOP)RuH(Cl)(CO) and **2** must proceed by a different mechanism than the PNN analog. We propose here a mechanism for the homogeneous catalysis with (PONOP)RuH(Cl)(CO) and with **2**, which is depicted in Scheme 6 and is based on the work of Milstein et. al., who studied the solution chemistry of this complex (46). In the first step, dehydrohalogenation of (PONOP)RuH(Cl)(CO) occurs with a base and generates a Ru(0)PONOP complex which functions as the active catalyst in the reaction. This complex was isolated by Milstein et. al. and was reported to be very reactive and unstable (46). Alcohol molecules then combine with Ru(0)PONOP in the second step and form a Ru(II)-hydride complex (Scheme 6). The next step is the formation of an aldehyde accompanied by formation of a ruthenium dihydride complex, which subsequently dehydrogenates to regenerate Ru(0)PONOP. The dihydride was also isolated by Milstein (46). As with the PNN the aldehyde compound reacts with another alcohol molecule to yield the hemiacetal intermediate, which, followed by a second cycle, produces esters with the liberation of hydrogen. The four-coordinate

Ru(0)PONOP and dihydride-Ru(II)PONOP complexes reported in the literature were P(^{i}Pr)$_3$ complexes instead of P(^{t}Bu)$_3$ [46]. As with **1**, we hypothesize that the amine functionality on the BP-1 surface is the base that gives the active catalyst, **2** (Scheme 6) [46,57].

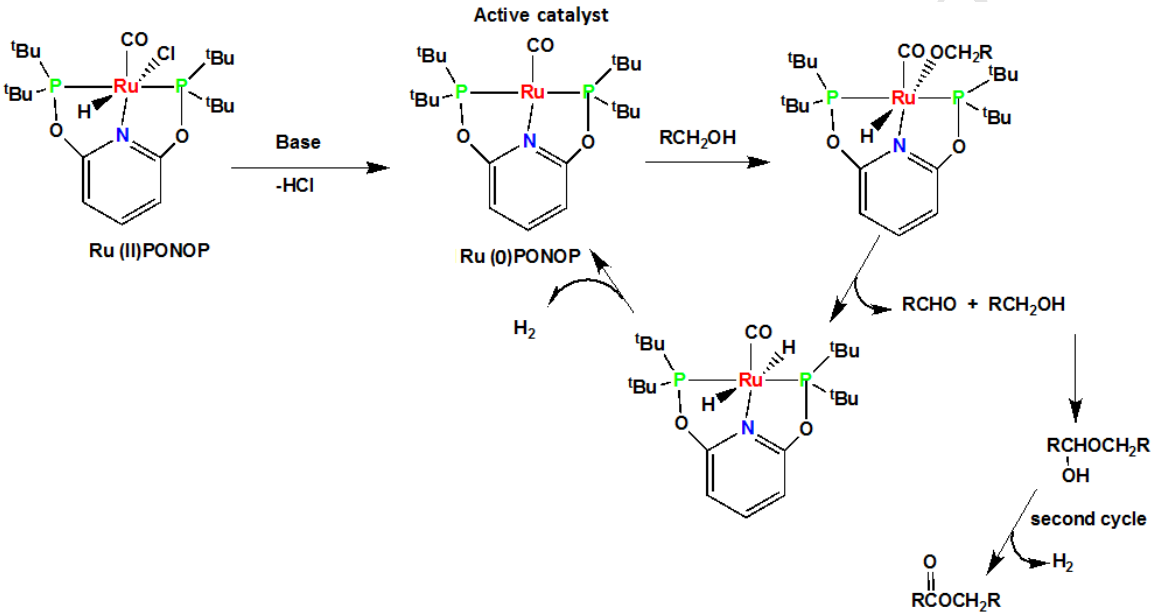

Scheme 6: A plausible mechanism for dehydrogenative coupling of alcohols to esters catalyzed (PONOP)RuH(Cl)(CO) or **2**.

It is not clear whether all immobilized (PONOP)RuH(Cl)(CO) was converted to the active catalytic species, Ru(0)complex, by the amines on the BP-1 surface during the loading of the complex on BP-1 or upon heating. As for **1**, FT-IR data was not very informative for elucidating the relative proportions of the original complex and the Ru(0) species on BP-1, since only one ν CO stretch was observed in the spectra for the metal carbonyl group. Our previous report on model solution experiments between Ru-PONOP and n-butyl amine indicated that the carbonyl stretching frequencies for the Ru-PONOP compound could be shifted significantly by the attachment of a group to the pyridine ring moiety of the complex [15]. In fact, upon immobilization of Ru-PONOP on BP-1, the metal carbonyl stretching frequency was found to be shifted by about 20 cm^{-1} [15]. However, we rationalized that there might not be considerable differences between the CO stretching frequencies of the original (PONOP)RuH(Cl)(CO) and the dehydrohalogenated active catalyst-(PONOP)Ru(CO) on BP-1 surfaces based on our previous results with the BP-1-Ru-PNN (**1**) system. Solid state CPMAS ^{13}C and ^{31}P NMR data were not very helpful in figuring out the relative ratio of both species on BP-1because of the broadness of the resonances.

3.4 Effect of solvents on the heterogeneous catalysis of alcohols with immobilized (PNN)RuH(Cl)(CO) and (PONOP)RuH(Cl)(CO) on BP-1

Reactions of 1-hexanol with both **1** and **2** in refluxing toluene under argon for 56 hours did not yield any esters using the same catalyst to substrate ratios reported for the homogeneous reaction (33). Addition of base to these heterogeneous reactions in refluxing toluene also resulted in no product formation, indicating that the heterogeneous reaction requires higher temperatures However, when the 1-heptanol reaction was carried out with **1** under reflux in the presence of 2 mL of dichlorobenzene, using a catalyst-to-alcohol ratio of 0.01:30 for 48 hours, under argon, 33% heptylheptanoate was formed. In the presence of 1 eq. KOH the reaction yield increased to 40%. The presence of solvent would be expected to decrease reaction rates in these heterogeneous (Table 3) [59-61].

3.5 Cycle study of dehydrogenative coupling of alcohols by 1 and 2 using solid-liquid and solid-vapor methods reaction configurations

The major advantage of heterogeneous catalysis is the facile recycling of important catalysts, offering the opportunity to reuse the catalysts in multiple cycles of reaction. In the case of the

SPC based catalysts **1** and **2** stirring of the reaction mixtures at elevated temperatures could degrade the catalyst particles. It was therefor decided to conduct the reactions by passing vapor over a bed of catalyst particles and to compare percent conversion with the solid-liquid stirred configuration over multiple cycles. No base was used in the cycle study and the substrate to catalyst ratios and reaction times were kept the same for both methods. Figure 3 depicts the reaction configuration for solid-liquid and solid-vapor methods. The cycle studies were carried out with three alcohols: 1-hexanol, 1-heptanol and benzyl alcohol. Conversions of alcohols in each of the cycles accompanied with turnover frequency with both **1** and **2** are presented in Tables 4 and 5.

The immobilized catalysts were characterized after catalytic reaction cycles by solid-state NMR (Figures 1s -11s). The amount of the complex remaining on BP-1 after catalysis was estimated by metal digestion studies as well as elemental analysis of the resulting composite catalysts. The results are shown in the Tables 5s and 6s.

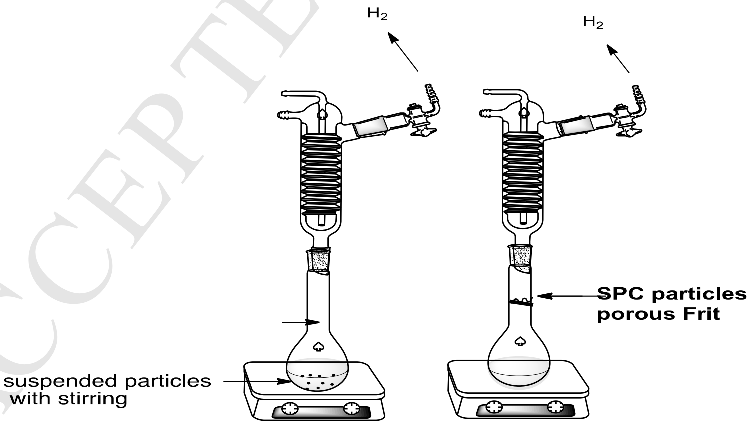

Figure 3: Schematic diagram for alcohol catalysis with the Solid-Liquid (left) and the Solid-Vapor (right) methods.

Catalyst **1** exhibited catalytic reactivity in the dehydrogenative coupling of alcohols up to five cycles, whereas **2** showed activity up to four catalytic cycles. In the first cycle, the conversion of alcohols to the corresponding esters was similar by both solid-liquid and solid-vapor methods, irrespective of the alcohol and catalyst used. On going from cycle 1 to 5 in the case of **1** and 1 to 4 in the case of **2**, alcohol conversion decreased considerably in both reaction configurations (Tables 4 & 5). The percentages of decrease in alcohol conversions varied from cycle to cycle with both immobilized systems irrespective of the alcohols and methods used (Tables 4 & 5). However, the solid-vapor method showed relatively better alcohol conversion in comparison to the solid-liquid method after the first cycle. This is likely due to the suggested particle degradation mentioned above. The decrease in ester yields from cycle 1 to 5 with BP-1-Ru-PNN and cycle 1 to 4 with BP-1-Ru-PONOP using both methods indicated that the catalysts leached off the BP-1 surface in each of the reaction cycles irrespective of the alcohols used. This was also evidenced by the loading of Ru-PNN and Ru-PONOP observed on the resulting composites (**1**) and (**2**) after catalysis (Tables 5s & 6s). The reaction yields were drastically decreased between cycles 3 to 4 (with both **1** and **2**) and 4 to 5 (with **1**) in comparison to cycles 1 to 2 and 2 to 3 (Tables 4, 5, 5s & 6s). Apparently catalyst leaching increased in the later cycles.

There was very good agreement between the reduction of alcohol conversions and the corresponding loss of the catalyst from BP-1 in the successive cycles for all three alcohols by both the solid-liquid and solid-vapor methods, which further indicates the leaching of the catalyst from the BP-1 surface during reactions. Turnover frequencies for alcohol catalysis on BP-1 were found to vary from cycle to cycle and were considerably lower than those observed in homogeneous reactions [33]. The decrease in alcohol conversion between two successive cycles was relatively lower in the 1-hexanol reaction compared to 1-heptanol and benzyl alcohol, which implies the relatively lower leaching of the complex with the lower boiling point of 1-hexanol (Tables 4 and 5). This is also supported by the higher loading of the complex found after the fifth cycle with 1-hexanol in the solid-vapor method, which was 0.015 mmol complex/gm BP-1 (Table 5s).

Table 4: Cycle study on dehydrogenative coupling catalysis with **1** using the solid-liquid (SL) and solid-vapor (SV) methods

Cycle	Alcohol	Reaction configuration	Reaction time (Hours)	Reaction temperature (°C)	Alcohol conversion (%)	Decrease in alcohol conversion between cycles (%)	Turnover frequency (Hour^{-1})
1-Hexanol	Cycle 1	Solid-Liquid	56	157	50	-	22
		Solid-Vapor	56	Alcohol vapor	51	-	23
	Cycle 2	Solid-Liquid	56	157	42	16	19
		Solid-Vapor	56	Alcohol vapor	47	8	21
	Cycle 3	Solid-Liquid	56	157	34	19	15
		Solid-Vapor	56	Alcohol vapor	41	12	18
	Cycle 4	Solid-Liquid	56	157	25	26	11
		Solid-Vapor	56	Alcohol vapor	36	12	16
	Cycle 5	Solid-Liquid	56	157	13	48	6
		Solid-Vapor	56	Alcohol vapor	26	28	12
1-Heptanol	Cycle 1	Solid-Liquid	48	176	52	-	33
		Solid-Vapor	48	Alcohol vapor	50	-	31
	Cycle 2	Solid-Liquid	48	176	35	32	22
		Solid-Vapor	48	Alcohol vapor	42	16	26
	Cycle 3	Solid-Liquid	48	176	21	40	13
		Solid-Vapor	48	Alcohol vapor	33	21	21
	Cycle 4	Solid-Liquid	48	176	10	52	6
		Solid-Vapor	48	Alcohol vapor	22	33	14
	Cycle 5	Solid-Liquid	48	176	5	50	3
		Solid-Vapor	48	Alcohol vapor	13	40	8
Benzyl alcohol	Cycle 1	Solid-Liquid	60	178	48	-	24
		Solid-Vapor	60	Alcohol vapor	52	-	26
	Cycle 2	Solid-Liquid	60	178	32	33	16
		Solid-Vapor	60	Alcohol vapor	43	17	22
	Cycle 3	Solid-Liquid	60	178	18	43	9
		Solid-Vapor	60	Alcohol vapor	34	21	17
	Cycle 4	Solid-Liquid	60	178	10	44	5
		Solid-Vapor	60	Alcohol vapor	21	38	11
	Cycle 5	Solid-Liquid	60	178	5	50	3
		Solid-Vapor	60	Alcohol vapor	12	42	6

Catalyst to alcohol ratio: 01:30 except in 1-hexanol where the ratio was 0.02:50.

Catalysts **1** and **2** lost their catalytic activity in each cycle by both methods, which was evidenced by the reduction of alcohol conversion observed in the corresponding catalytic cycles (Tables 4, 5). In some cases, the reduction in alcohol conversion between two successive reaction cycles was relatively lower than the corresponding loss or degradation of the catalyst on the BP-1 surface as estimated from Ru analysis (Tables 5s & 6s). This could be due to the formation of more deprotonated Ru-PNN species on BP-1 in the repeated cycles of catalysis.

All of the data reported here indicates that (PONOP)RuH(Cl)(CO) complex is comparatively less stable than (PNN)RuH(Cl)(CO) in the catalytic reactions and decomposes faster.

FT-IR spectra of the resulting composite, **1** after catalysis showed a metal carbonyl stretch at 1944 cm^{-1}, which was very similar to that observed in the original immobilized catalyst before catalysis (1948 cm^{-1}). This confirmed the presence of Ru-PNN on BP-1 after catalysis. However, IR data from cycles 3 to 5 were not very informative because of the low abundance of the complex on BP-1. A good correlation was also realized between the results of phosphorus and Ru-analysis of the resulting composite after catalysis, which gives further evidence of the existence of Ru-PNN and Ru-PONOP on BP-1 after catalysis. Slightly higher percentages of carbon and hydrogen were observed in the elemental analysis of BP-1-Ru-PNN (**1**) and BP-1-Ru-PONOP (**2**) catalysts after catalysis in comparison to those observed before catalysis, which could be due to the unreacted alcohols and/or product esters remaining on the composite after washing. Solid-state ^{13}C NMR spectra of **1** after catalysis displayed expected resonances for pyridine carbons at δ 162.5 and for the *tert*-butyl and ethyl carbons of the complex at δ 22.1 and 62.3 ppm respectively which were very similar to those observed for the complex on BP-1 before catalysis. This suggested that the Ru-PNN complex remained intact on BP-1 after catalysis. However, the relative intensity of resonances decreased in the CPMAS ^{13}C NMR spectra of the resulting composite going from cycle 1 to 3 (Figures 9S, 10S, 11S). This demonstrated the gradual leaching of the complex from the BP-1 surfaces after each cycle of the reaction, consistent with the relative decrease of the alcohol conversions noticed from cycle to cycle (Tables 4 and 5s).

FT-IR spectra of **2** after catalysis showed the expected metal carbonyl stretching frequency at 1956 cm^{-1}, which was similar to that observed before catalysis (1952 cm^{-1}) [15], confirming the presence of the complex on BP-1 after catalysis. However, after cycles 3 and 4, FT-IR spectra were not very informative since the ν CO stretch was too weak because of the low abundance of the complex on the resulting composites. There was no Ru content found on the resulting composite **2** with the solid-liquid method after the 4th catalytic cycle, which showed that the loaded Ru-PONOP completely decomposed or leached off with the repeated catalytic cycles (Table 5 and 6s).

In the solid vapor experiments, only the surface amines activate catalyst, no KOH was used. The vapor reaching the reactive zone in the solid-vapor experiments must be very close to the boiling point of the alcohol under vigorous reflux conditions. After passing through the glass frit on, which the catalyst sits, the vapor condenses and must be at an undetermined lower temperature when it passes through the frit again. It is not possible to determine if the condensed vapor contributes to the catalytic process.

Table 5: Cycle study on alcohol catalysis on **2** using the solid-liquid (SL) and solid-vapor (SV) methods

Cycle	Alcohol	Reaction configuration	Reaction time (Hours)	Reaction temperature (°C)	Alcohol conversion (%)	Decrease in alcohol conversion between cycles (%)	Turnover frequency (Hour^{-1})
1-Hexanol	Cycle 1	Solid-Liquid	56	157	43	-	22
		Solid-Vapor	56	Alcohol vapor	41	-	23
	Cycle 2	Solid-Liquid	56	157	32	16	19
		Solid-Vapor	56	Alcohol vapor	35	8	21
	Cycle 3	Solid-Liquid	56	157	20	19	15
		Solid-Vapor	56	Alcohol vapor	26	12	18
	Cycle 4	Solid-Liquid	56	157	10	26	11
		Solid-Vapor	56	Alcohol vapor	16	12	16
1-Heptanol	Cycle 1	Solid-Liquid	48	176	55	-	33
		Solid-Vapor	48	Alcohol vapor	51	-	31
	Cycle 2	Solid-Liquid	48	176	37	32	22
		Solid-Vapor	48	Alcohol vapor	42	16	26
	Cycle 3	Solid-Liquid	48	176	20	40	13
		Solid-Vapor	48	Alcohol vapor	27	21	21
	Cycle 4	Solid-Liquid	48	176	7	52	6
		Solid-Vapor	48	Alcohol vapor	14	33	14
Benzyl alcohol	Cycle 1	Solid-Liquid	60	178	49	-	24
		Solid-Vapor	60	Alcohol vapor	47	-	26
	Cycle 2	Solid-Liquid	60	178	28	33	16
		Solid-Vapor	60	Alcohol vapor	35	17	22
	Cycle 3	Solid-Liquid	60	178	16	43	9
		Solid-Vapor	60	Alcohol vapor	24	21	17
	Cycle 4	Solid-Liquid	60	178	4	44	5
		Solid-Vapor	60	Alcohol vapor	12	38	11

Catalyst to alcohol ratio: 01:30 except in 1-hexanol where the ratio was 0.02:50.

Solid-state CPMAS ^{13}C NMR spectra of **2** after catalysis showed the expected resonances for pyridine carbons at δ 163.3 and the resonance for *tert*-butyl carbons appeared at δ 25.3, which were very similar to those observed for the immobilized Ru-PONOP before catalysis (Figures 2S & 6S) [15]. This suggests that some of the complex retained its structure on BP-1 even after catalysis. In addition, solid state CPMAS ^{31}P NMR spectra displayed a resonance at δ 50.3 ppm which was very close to that observed for BP-1-Ru-PONOP (**2)** (δ 58 ppm) before catalysis. This further confirmed the presence of Ru-PONOP on BP-1 after catalysis. In addition, a second ^{31}P resonance was observed at δ 72 ppm and suggested the presence of Ru(0)PONOP complex on

BP-1 (Figure 5S). However, the intensity of the resonances in the solid-state CPMAS ^{13}C NMR decreased from cycles 1 to cycle 3, which can be attributed to the leaching of the Ru-PONOP from the BP-1 surfaces as the composite catalyst was recycled for multiple runs of the reactions (Figures 6S, 7S & 8S).

3.6 Control experiments between 1-hexanol and immobilized pincer complexes on BP-1

It was quite clear that the decreases in reaction yields in the multiple cycles of catalytic reactions with 1-hexanol, 1-heptanol, and benzyl alcohol were due to the leaching or decomposition of catalysts from the BP-1 surfaces. These observations led to a major concern: whether the alcohol catalysis occurring on BP-1 surfaces was truly heterogeneous in nature or whether the complexes leached off the BP-1 surfaces into solution at the beginning of the reactions and then performed catalysis. There is a lot of controversy regarding heterogeneous catalytic processes on a solid surface with immobilized catalysts, particularly when leaching or decrease of catalyst performance were observed in repeated reaction cycles [31-32, 63-64]. In the present catalytic study, we considered two possibilities: (i) immobilized catalyst remained on the BP-1 surfaces during catalysis and performed alcohol catalysis on the surfaces, then leached off or decomposed at the end of the catalytic reactions, and (ii) immobilized catalysts leached from the BP-1 surfaces at the beginning of the catalytic reactions and mixed with reactant alcohols and the catalysis was then accomplished in the solution phase. To clarify these possibilities and to better understand the catalytic processes occurring on the BP-1 surface with immobilized catalysts, control experiments were carried out using 1-hexanol in the absence of a base and with the addition of 1 eq. of KOH.

The control experiments involved four-steps. In the first step, the mixture of 1-hexanol and **1** was stirred at room temperature under argon for 4-5 hours. The resulting liquid mixture was tested by GC-MS. No conversion of alcohol was observed in this step, showing that catalysis on did not occur at room temperature. In step 2, 1-hexanol and **1** were heated at 157°C under argon for about 16 hours. A 30% yield of hexylhexanoate was realized. Thus high reaction temperatures are required for dehydrogenative catalysis with **1**. In step 3, the resultant reactant mixture from step 2 was heated further at 157°C for about 3-4 hours, and an additional 4% conversion of 1-hexanol was found. This result indicated that some active catalyst was still present. After step 3, the liquid mixture was separated from **1**. Then the resultant liquid mixture was heated at 157°C for 15 hours under argon in the absence of **1**. GC-MS analysis on the product mixture from step 4 showed only 2-3% conversion, which clearly showed that leached Ru-PNN complexes were not active catalysts, otherwise considerable conversion of 1-hexanol should have been realized at this stage. These experiments do not prove that the catalysis is strictly heterogeneous in nature but does confirm that leached complex is not the active catalyst. There are two possible scenarios: 1) catalysis occurs on the surface but the catalytically active complex decomposes after a few turnovers; 2) Activated catalyst leaches from the surface, performs catalysis in solution and then decomposes after a few turnovers. When the same control experiment was carried out in the presence of 1 equivalent of KOH, following steps 1 to 4, similar results were observed in each of the steps except the formation of relatively more ester yield (36%) in step 2 compared to that reported above. That the bulk of catalysis occurs in the first 25-30 hours is consistent with the idea that immobilized complex is the launch point for catalysis. The most compelling argument for this is the correlation between conversion and the amount of catalyst remaining on the surface and of course the apparent activation of catalyst on the amine surface. These same control experiments gave similar results when conducted with **2**

4. Conclusions

(PNN)RuH(Cl)(CO) and (PONOP)RuH(Cl)(CO) pincer complexes were covalently immobilized on BP-1. The presence of the complex on BP-1 was confirmed by characterization with the standard spectroscopic techniques, FT-IR, solid-state NMR, elemental analysis, and metal digestion. The model solution experiments between (PNN)RuH(Cl)(CO) and n-butyl amine showed the formation of both *meta*- and *para*- isomers, indicating the position of the electrophilic substitution at the pyridine ring of the pincer complexes during loading on BP-1. The pincer arms of the mixture of products were deprotonated with KO^{t}Bu generating dearomatized-Ru-PNN-n-butyl amine as the active catalyst complex. Dehydrogenative coupling catalysis with this complex gave lower alcohol conversion in comparison with the original deprotonated catalyst (PNN)RuH(CO) demonstrating that substitution on the pyridine ring decreases catalytic performance of the Ru-PNN pincer complex [50].

Dehydrogenative coupling of four alcohols was investigated with **1** and **2** and all gave moderate dehydrogenative coupling yields except the secondary alcohol, 2-octanol, even without added base, a strict requirement for the analogous homogeneous reaction [33]. This suggests that surface-bound amine functionality on BP-1 functions as a base to generate active pincer catalytic complex on the BP-1 surface. Yields were lower but catalysis worked at lower substrate to catalyst ratios (0.03%) than in the homogeneous systems where 0.1 mol % catalyst was used.

The (PONOP)RuH(Cl)(CO) pincer complex exhibited catalytic reactivity toward dehydrogenative coupling of alcohols to esters in both homogeneous reactions and with the SPC immobilized complexes. As for the PNN system no added base was required with the latter. A mechanism was proposed for alcohol dehydrogenative coupling reactions by (PONOP)RuH(Cl)(CO), which involved the generation of Ru(0) complex that reacted with alcohol, and then catalysis proceeded with the formation of a ruthenium dihydride complex (Scheme 6). Both of these proposed intermediate complexes were actually isolated by Milstein et. al. (46) Overall, the catalytic performance of (PONOP)RuH(Cl)(CO) was not as good as the (PNN)RuH(Cl)(CO).

Both immobilized Ru-PNN and Ru-PONOP catalysts on BP-1 were reused for multiple cycles in dehydrogenative coupling reactions. Catalyst **1** showed activity for up to five catalytic cycles, whereas **2** survived up to the fourth cycle of catalysis. Better performance was realized in these cycles when a vapor-solid reaction system was used as this avoided particle degradation during stirring.

Both catalysts showed a good correlation between the decease in yield from cycle to cycle and the amount of catalyst leached from the surface. A series of control experiments showed that leached catalyst is not active. This lead us to the conclude that activation of the catalysts by surface amines occurs heterogeneously and then catalysis occurs on the surface or after the activated catalyst leaches from the surface with decomposition occurring after a few turnovers in either case. Based on all the analytical and spectroscopic data we can exclude the possibility of Ru nanoparticles as the active catalyst. SEM images before and after binding of the complexes to the SPC showed no significant changes in morphology of the particles (Figure 12S).

For these systems to become useful, catalysis must be achieved at much lower temperatures to avoid leaching/decomposition. Higher catalyst loading must be achieved for this to become a reality. This study does demonstrate that polyamines could prove very important surfaces for activating catalysts that require base to generate the catalytically active species. In addition, the homogeneous model studies demonstrate the impact of ring substitution on catalytic activity and carbonyl stretching frequencies.

Acknowledgement

The authors gratefully acknowledge the support of Grant from the National Science Foundation (CHE-1049567). The authors are indebted with JEOL Company for helpful technical assistance and cooperation.

References

[1] N.C. Mehendale, C. Bezemer, C.A. van Walree, , R.J.M.K. Gebbink, G. van Koten, J. Mol. Catal. A: Chem. 257 (2006) 167–175.

[2] B. Cornils, W.A. Herrmann, J. Catal. 216 (2003) 23-31.

[3] V. Udayakumar, S. Alexander, V. Gayathri, V. Shivakumaraiah, K.R. Patil, B. Viswanathan, J. Mot. Catal. A Chem. 317 (2010) 111−117.

[4] B.H.G. Swennenhuis, R. Chen, P.W.N.M. van Leeuwen, J.G. deVries, P.C.J. Kamer, Eur. J. Org. Chem. 33 (2009) 5796−5803.

[5] E. Karakhanov, A. Maximov, in: D. Wohrle, A. Pomogajlo (Eds.), Metal Complexes and Metals in Macromolecules, John Wiley & Sons, New York, 2003, p. 457.

[6] E. Karakhanov, A. Maximov, Y. Kardasheva, V. Semernina, A. Zolotukhina, A. Ivanov, G. Abbott, E. Rosenberg, ACS Appl. Mater. Interfaces 6 (2014) 8807−8816.

[7] G. Abbott, R. Brooks, E. Rosenberg, M. Terwilliger, J.B. Alexander Ross, O.L. Ichire, Organometallics 33 (2014) 2467−2478.

[8] B. Tamami, M.M. Nezhad, S. Ghasemi, F. Farjadian, J. Organomet. Chem. 743 (2013) 10−16.

[9] M. Berlin, J. Allen, V. Kailasam, D. Rosenberg, E. Rosenberg, Appl. Organometal. Chem. 25 (2011) 530−536.

[10] H.U. Blaser, B. Pugin, M. Studer, in: D.E. De Vos, I.F.J. Vankelecom, P.A. Jacobs (Eds.), Chiral Catalyst Immobilization and Recycle, VCH, Weinheim, 2000, p. 9.

[11] C.W. Jones, M.W. McKittrick, J.V. Nguyen, K. Yu, Top. Catal. 34 (2005) 67−76.

[12] H.U. Blaser, B. Pugin, M. Studer, in :Chiral Catalyst Immobilization and Recycle, eds. De Vos, D.E.; Vankelecom, I.F.J.; Jacobs, P.A. (VCH, Weinheim, 2000) p. 9.

[13] A.H. Gemeay, A.B. Zaki, M.Y. El-Sheikh, H.F. El-Saied, Transition Met. Chem. 28 (2003) 625-631.

[14] C.D. Pozo, A. Corma, M. Iglesias, F. Sanchez, Organometallics 29 (2010) 4491.

[15] M.A. Goni, E. Rosenberg, S. Meregude, G. Abbott, J. of Organomet. Chem. 807 (2016), 1-10.

[16] K. Arashiba, Y. Miyake, Y. Nishibayashi, Nat. Chem. 3 (2011) 120−125.

[17] R. Tanaka, M. Yamashita, K. Nozaki, J. Am. Chem. Soc. 131 (2009) 14168−14169.

[18] S. Chakraborty, J.A. Krause, H. Guan, Organometallics 28 (2009) 582−586.

[19] D. Morales-Morales, C. Jensen, The Chemistry of Pincer Compounds, Elsevier Science, Amsterdam, 2007.

[20] A.S. Goldman, A.H. Roy, Z. Huang, R. Ahuja, W. Schinski, M. Brookhart, Science 312 (2006) 257−261.

[21] M Albrecht, G. van Koten Angew. Chem. Int. Ed. Engl. 40 (2001) 3750

[22] P.A. Chase, R.J.M. Klein Gebbink, G. van Koten, J. Organomet. Chem. 689 (2004) 4016−4054.

[23] J.W.J. Knapen, A.W. van der Made, J.C. de Wilde, P.W.M.N. van Leeuwen, P. Wijkens, D.M. Grove, G. van Koten, Nature (1994) 372.

[24] D.E. Bergbreiter, P.L. Osborn, J.D. Frels, J. Am. Chem. Soc. 123 (2001) 11105−11106.

[25] N.C. Mehendale, J.R.A. Sietsma, K.P. de Jong, C.A. van Walree, R.J.M.K. Gebbink, G. van Koten, Adv. Synth. Catal. 349 (2007) 2619−2630.

[26] A.R. McDonald, H.P. Dijkstra, B.M.J.M. Suijkerbuijk, G.P.M. van Klink, G. van Koten, Organometallics 28 (2009) 4689−4699.

[27] W.J. Sommer, K. Yu, J.S. Sears, Y. Ji, X. Zheng, R.J. Davis, C.D. Sherrill, C.W. Jones, M. Weck, Organometallics 24 (2005) 4351−4361.

[28] Z. Huang, M. Brookhart, A.S. Goldman, S. Kundu, A. Ray, S.L. Scott, B.C. Vicente,

Adv. Synth. Catal. 351 (2009) 188−206.

[29] B.C. Vicente, Z. Huang, M. Brookhart, A.S. Goldman, S.L. Scott, Dalton Trans. 40 (2011) 4268−4274.

[30] M. Rimoldi, D. Fodor, J.A. van Bokhoven, A. Mezzetti, Chem. Commun. 49 (2013) 11314−11316.

[31] K Yu, W. Sommer, M. Weck, C.W. Jones, J. Catal. 226 (2004) 101−110.

[32] K. Yu, W. Sommer, J.M. Richardson, M. Weck, C.W. Jones, Adv. Synth. Catal. 347 (2005) 161−171.

[33] J. Zhang, G. Leitus, Y. Ben-David, D. Milstein, D. J. Am. Chem. Soc. 127 (2005) 10840-10841.

[34] D. Milstein, Top. Catal. 53 (2010) 915–923.

[35] T. Chen, L. Yang, L. Li, K-W. Huang, Tetrahedron 68 (2012) 6152-6157.

[36] R. Langer, Y. Diskin-Posner, G. Leitus, L.J.W. Shimon, Y. Ben-David, D. Milstein, Angew. Chem. Int. Ed. 50 (2011) 9948−9952.

[37] P. Kang, C. Cheng, Z. Chen, C.K. Schauer, T.J. Meyer, M. Brookhart, J. Am. Chem. Soc. 134 (2012) 5500−5503.

[38] N. Selander, K.J. Szabo, Chem. Rev. 111 (2011) 2048−2076.

[39] M. Hughes, D. Nielsen, E. Rosenberg, R. Gobetto, A. Viale, S.D. Burton, Ind. Eng. Chem. Res. 45 (2006) 6538.

[40] S.T. Beatty, R.J. Fischer, D.L. Hagers, E. Rosenberg, Ind. Eng. Chem. Res. 38 (1999) 4402−4408.

[41] Y.O. Wong, P. Miranda, E. Rosenberg, J. Appl. Poly. Sci. 115 (2010) 2855−2864.

[42] M. Hughes, Paul Miranda, D. Nielsen, E. Rosenberg, R. Gobetto, A. Viale, S. Burton, Silica polyamine composites: new supramolecular materials for cation and anion recovery and remediation, in: R. Barbucci, F. Ciardelli, G. Ruggeri (Eds.), Recent Advances and Novel Approaches in Macromoleculemetal Complexes, Wiley- VCH, Weinheim, 2006, p. 161 (Macromolecular Symposia 235).

[43] S. Nishimura, Handbook of Heterogeneous Catalytic Hydrogenation for Organic synthesis, John Wiley & Sons, New York, 2001.

[44] J.M. Thomas, J. Mol. Catal. A Chem. 146 (1999) 77−85.

[45] J. Allen, E. Rosenberg, E. Karakhanov, S.V. Kardashev, A. Maximov, A. Zolotukhina,

Appl. Organometal. Chem. 25 (2011) 245−254.

[46] H. Salem, L.J.W. Shimon, Y. Diskin-Posner, G. Leitus, Y. Ben-David, D. Milstein, Organometallics 28 (2009) 4791–4806.

[47] A. Goni, E. Rosenberg, in: Abstracts 2016 ACS National Meeting held in Philadelphia PA, August 20-25, 2016. Abstract # 2517419.

[48] S. Kundu, W.B. Willium, W.D. Jones, Inorg. Chem. 50 (**2011)** 9443.

[49] a) M. Q. Slagt, G. Roddriguez, M. M.P. Grutters, M. M. P. Gebbink, R. J. M. KleinW. Klopper, L. W. Jenneskens, M. S. Lutz, A. L. Spek, G. Van Koten Chem. Eur. J. 10 (2004) 1331. b) G. D. Batema, M. Lutz, A. L. Spek, C. A. van Wairee, G. P. M. van Klink, G. Van Koten Dalton Trans. 43 (2014) 12200.

[50] a) L. A. van der Kuil, H. Luitjes, D. M. Grove, J. W. Zwikker, J. G. M. van der Linden,A. M. Roelofsen, L. W. Jenneskens, W. Drenth, G. van Koten Organometallcs 13 (1994) 468. b) M. Gagliardo, D. J. M. Sneiders, P. A. Chase, M. M. P. Gebbink K. van Klink, G. van Koten Angew Chem. Int. Ed. Engl. 46, (2007) 8558.

[51] W. DeRieux, A. Wong, Y. Schrod, J. Organomet. Chem. 772 (2014) 60-67.

[52] C. Gunanathan, Y. Ben-David, D. Milstein, Science 317 (2007) 790-792.

[53] R. Langer, G. Leitus, Y. Ben-David, D. Milstein, Angew. Chem. Int. Ed. 50 (2011) 2120–2124.

[54] E. Balaraman, C. Gunanathan, J. Zhang, L.J.W. Shimon, D. Milstein, Nat. Chem. 3 (2011) 609-614.

[55] J. Zhang, M. Gandelman, J.W. Linda, L.J.W. Shimon, D. Milstein, Dalton Trans. (2007) 107–113.

[56] B. Gnanaprakasam, E. Balaraman, Y. Ben-David, D. Milstein, Angew. Chem. Int. Ed. 50 (2011) 12240 –12244.

[57]. B. Gnanaprakasam, Y. Ben-David, D. Milstein, Adv. Synth. Catal. 352 (2010) 3169 – 3173.

[58] B. Gnanaprakasam, D. Milstein, J. Am. Chem. Soc. 133 (2011) 1682–1685.

[59] E. Balaraman, Y. Ben-David, D. Milstein, Angew. Chem. Int. Ed. 50 (2011) 11702 –11705.

[60] A. Goni, E. Rosenberg, in: Abstracts 2015 ACS Northwest Regional Meeting held in Pocatello, ID, June 21-24, 2015. Abstract # 33.

[61] L. Gilbert, C. Mercier, Studies in Surfaces Science and Catalysis 78 (1993) 51-66.

[62] B.S. Akpa, C.D. Agostino, L.F. Gladden, K. Hindle, H. Manyar, J. McGregor, R. Li, M. Neurock, N. Sinha, E.H. Stitt, D. Weber, J.A. Zeitler, D.W. Rooney, J. of Catal. 289 (2012) 30-41.

[63] A. Choplin, F. Quignard, Coord. Chem. Rev. 178-180 (1998) 1679-1702.

[64] J.M. Richardson, C.W. Jones, J. Mol. Catal. A: Chem. 297 (2009) 125–134.

Highlights for:

Dehydrogenative Coupling of Alcohols to Esters on a Silica Polyamine Composite by Immobilized PNN and PONOP Pincer Complexes of Ruthenium

by

Md Abdul Goni and Edward Rosenberg[*]

Department of Chemistry and Biochemistry, University of Montana, Missoula MT

59812

and

Roberto Gobetto and Michele Chierotti

Dipartimento di Chimica IFM, Universitá di Torino, via P. Giuria 7, 10125,Turin,

Italy

1. Two Ru pincer complexes have been immobilized on a silica polyamine composite and are shown to be active catalysts for dehydrogenative coupling of alcohols.
2. The amine surface provides the required base needed to activate the complexes for the catalysis.
3. Model reactions studied in solution show the regiochemistry of electrophilic aromatic substitution with both para-and meta isomers being formed.
4. Catlyst leaching proved to be a problem but conversions could be obtained up to 5 cycles.